Journal of Molecular Structure 919 (2009) 154–159

Contents lists available at ScienceDirect

Journal of Molecular Structure

journal homepage: www.elsevier.com/locate/molstruc

Structure, antibacterial activity and theoretical study of 2-hydroxy-1-naphthaldehyde-*N*-methylethanesulfonylhydrazone

Neslihan Özbek [a], Gülten Kavak [b], Yusuf Özcan [c], Semra İde [c], Nurcan Karacan [d,*]

[a] Department of Primary Education, Faculty of Education, Ahi Evran University, 40100 Kırşehir, Turkey
[b] Department of Physics, Faculty of Science and Art, Dicle University, 21280 Diyarbakır, Turkey
[c] Department of Physics Engineering, Faculty of Engineering, Hacettepe University, 06800 Beytepe, Ankara, Turkey
[d] Department of Chemistry, Science and Art Faculty, Gazi University, 06500 Ankara, Turkey

ARTICLE INFO

Article history:
Received 21 July 2008
Received in revised form 27 August 2008
Accepted 8 September 2008
Available online 20 September 2008

Keywords:
Crystal structure
Sulfonyl hydrazones
Antimicrobial activity
Conformation
Tautomerism

ABSTRACT

2-Hydroxy-1-naphthaldehyde-*N*-methylethanesulfonylhydrazone was synthesized and its structure was investigated by X-ray diffraction, IR, NMR and mass spectroscopies. It crystallizes in the monoclinic system, space group $P2_1/c$, a = 22.712(4), b = 5.793(4), c = 11.032(2) Å, α = 90.0, β = 102.070(8)°, γ = 90.0°, V = 1419.4(1) Å^3, Z = 4. Spectroscopic assignment and calculations carried out using B3LYP/6-31G** basis set and crystallographic results indicate the predominance of the phenol-imine tautomeric form. It has strong intramolecular hydrogen bond of type O—H N [with distance donor–acceptor 2.579(4) Å]. The angular disposition of the bonds about the sulfur atom significantly deviates from that of a regular tetrahedron as expected. This deviation can be attributed to the non-bonded interactions involving the S=O bonds and methyl groups in both molecular and crystal structure. Result of conformational analysis was also compared with crystallographic data. Antimicrobial activity of the title compound was screened against *E. coli* ATCC 11230, *P. aeruginosa* ATCC 28753, *S. enteritidis* ATCC 40376, *S. aureus* ATCC 25923 and *B. cereus* RSKK 863.

1. Introduction

Sulfonyl hydrazones are found to be reported in limited researches in the literature in spite of being derivatives of sulfonamide exhibiting large medicinal applications. Similar to sulfonamides [1–5], sulfonyl hydrazones also have various biological activities. For example, imidosulfonylhydrazones have antibacterial and antineociceptive properties [6]. Acidic sulfonyl hydrazones derivatives have analgesic and anti-inflammatory activities [7]. Benzaldehyde arylsulfonylhydrazones possess antineoplastic activity against human stomach cancer SGC 7901 [8]. 4-Substituted benzenesulfonylhydrazone has been found to have antibacterial activity [9]. *N*-arylsulfonyl hydrazones have been identified as novel inhibitors of IMP-1 a metallo-β-lactamase enzyme [10].

In our previous studies, synthesis and theoretical study of methanesulfonic acid hydrazide was performed [11]. Sulfonyl hydrazone derivatives were synthesized and screened for antimicrobial and cytotoxic activity [12]. Synthesis of metal carbonyl complexes of the sulfonyl hydrazones were also reported [13–19]. Furthermore, aliphatic and aromatic disulfonamides were synthesized and evaluated for antimicrobial activity [20–22]. As part of our ongoing studies, the title compound (Fig. 1) was synthesized and its structure was determined by X-ray diffraction method, IR, NMR and mass spectrocopies. Tautomerism and conformational analysis of it were carried out by quantum chemical methods. In addition, antimicrobial activity of the title compound was screened against pathogen bacterias, such as *E. coli* ATCC 11230, *P. aeruginosa* ATCC 28753, *S. enteritidis* ATCC 40376, *S. aureus* ATCC 25923 and *B. cereus* RSKK 863.

2. Experimental and computational methods

2.1. Physical measurements

Reagents were obtained commercially from Aldrich (ACS grade) and used as received. All extracted solvents (all from Merck) were dried over anhydrous Na_2SO_4 and evaporated with a BUCHI rotary evaporator. The elemental analyses (C, H, N and S) were performed on a LECO–CHSNO-9320 type elemental analyzer. The IR spectra (4000–400 cm^{-1}) were recorded on a Mattson-1000 FT-IR spectrophotometer with samples prepared as KBr pellets. NMR spectra were recorded on a Bruker-Spectrospin Avance DPX-400 UltraShield (400 MHz) using DMSO-d_6 and $CDCl_3$ as a solvent and TMS as an internal standard. The melting point was recorded on an OptiMelt apparatus.

* Corresponding author. Tel.: +90 3122021117; fax: +90 3122122279.
E-mail address: nkaracan@gazi.edu.tr (N. Karacan).

0022-2860/$ - see front matter © 2008 Elsevier B.V. All rights reserved.
doi:10.1016/j.molstruc.2008.09.010

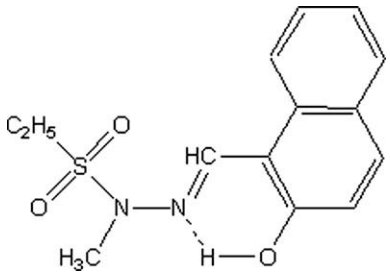

Fig. 1. The structure of the title compound.

2.2. Synthesis

Ethanolic solution of ethanesulfonic acid 1-methylhydrazide (0.62 g, 4.46 mmol) was added dropwise to an ethanolic solution of 2-hydroxy-1-naphthaldehyde (1.15 g, 6.7 mmol), maintaining the temperature at about −5 °C. Then, the mixture was stirred for 5 h at room temperature. The precipitated product was crystallized from ethanol/*n*-hexane mixture. The yellow crystalline solid was dried in vacuo and stored at ethanol/*n*-hexane vapor. Yield 66%; mp 164–165 °C.

IR (KBr) cm^{-1}: 1621 υ (C=N), 1240 υ(C—O), 1340 υ_{as} (SO_2), 1183 υ_s (SO_2); ^1H NMR (d_6-DMSO) δ: 1,44 ppm (t, 3H, CH_3), 3,26 ppm (q, 2H, CH_2), 3,52 ppm (s, 3H, N—CH_3), 8,78 ppm (s,1H, N=CH), 10,45 ppm (s, 1H, OH), 7.28–8.04 ppm (m, ArH); ^{13}C NMR (d_6-DMSO) δ: 8,12 ppm (CH_3), 44,54 ppm (CH_2), 33.04 ppm (N—CH_3), 157,28 ppm (N=CH); 109.77–132.79 ppm (ArC); EIMS (70 eV) *m*/*z*: 292 (M^+, 12.5%, M+1, 2.6%); Anal. Calcd. for $C_{14}H_{16}SO_3N_2$: C, 57.52; H, 5.47; N, 9.56; S, 10.97. Found: C, 57.65; H, 5.13; N, 10.07; S, 10.63.

2.3. Crystal structure determination

The X-ray structural study of the title compound has been carried out in order to obtain the certain structural information about the ethanesulfonylhydrazone. The details about the measurements and crystallographic studies are given in Table 1. Diffraction data were collected on Enraf-Nonius CAD4 diffractometer with graphite monochromated MoKα (0.71073 Å) radiation [23]. The structure was solved by direct methods and refined by least squares on F^2 using SHELXS-97 and SHELXL-97 software packages, respectively [24]. The non-hydrogen atoms were refined anisotropically. H2'(O1) and H11(C11) hydrogens were located in difference syntheses and refined isotropically [O—H = 0.90(4) Å, Uiso(H) = 0.087(13) Å2 and C—H = 0.910(17) Å, Uiso(H) = 0.045(7) Å2]. The remaining H atoms were positioned geometrically with C—H = 0.93, 0.97 and 0.96 Å for aromatic, methylene and methyl H, respectively, and constrained to ride on their parent atoms with Uiso(H) = *x*Ueq(C), where *x* = 1.5 for methyl H and *x* = 1.2 for all other H atoms. The final atomic coordinates and equivalent isotropic displacement parameters of the nonhydrogen atoms are given in Table 2.

2.4. Method of calculation

Initial geometry of structure was taken from crystal data. An extensive search for low energy conformations on the potential energy surface (PES) of the compound was carried out by using a systematic search with RHF/6-31G** levels. Obtained minimum energy conformations were reoptimized at DFT/B3LYP/6-31G** levels without symmetry constraint. Minima, as well as transition states, were characterized through harmonic frequency analysis. All the calculations reported here were carried out with the GAUSSIAN03 software [25] employing standard basis sets with no modifications. Quantum chemical descriptors (HOMO, LUMO, dipole moment, heat of formation) for tautomers were calculated after B3LYP/6-31** method with the same software. Surface area (approx) and molecular volume of compound were calculated by using the Hyperchem (release 7.5) package program [26].

2.5. Antibacterial assay

Escherichia coli ATCC 11230, *P. aeruginosa* ATCC 28753, *S. enterititis* ATCC 40376, *S. aureus* ATCC 25923, *B. cereus* RSKK 863 cultures were obtained from Gazi University, Biology Department and Refik Saydam Hygiene Center Culture Collection. Bacterial strains were cultured overnight at 37 °C in Nutrient Broth. These stock cultures were stored in the dark at 4 °C during the survey.

Bacterial susceptibility testing was performed by the disc diffusion method according to the guidelines of Clinical and Laboratory Standards Institute (CLSI) [27]. The sterilized (autoclaved at 120 °C

Table 1
Crystallographic details of the title compound

Crystal formula	$C_{14}H_{16}N_2O_3S$
Formula weight	292.4
Crystal dimensions (mm)	0.40 × 0.30 × 0.20
Temp (K)	291(2)
Crystal system	Monoclinic
Space group	$P2_1/c$
a (Å)	22.712(4)
b (Å)	5.793(4)
c (Å)	11.032(2)
α (°)	90.0
β (°)	102.1(1)
γ (°)	90.0
V (Å^3)	1419.4(1)
Z; D_{calc}, (g cm^{-3})	4; 1.37
F(000)	615.9
Range of θ (°)	3.6/26.3
μ (MoK_α) (mm^{-1})	0.237
Reflections collected	5759
Reflections used in refinement	2874
No. of refined parameters	189
R/R_w values	0.0562/0.1765
GOF	1.0040
Final shift	0.000
$(\Delta\rho)_{min}$, $(\Delta\rho)_{max}$ (e Å^{-3})	−0.426, 0.510

Table 2
Fractional atomic coordinates and equivalent isotropic displacement parameters (Å^2) for the title compound

Atom	*x*	*y*	*z*	U(eq) [Å^2]
O1	0.2459(1)	1.0567(4)	0.1180(2)	0.0607(6)
O2	0.0803(1)	0.3256(4)	0.0101(3)	0.0840(9)
O3	0.1449(1)	0.5644(5)	0.1694(2)	0.0819(8)
N1	0.2090(1)	0.6934(4)	−0.0106(2)	0.0477(6)
N2	0.1676(1)	0.5188(4)	−0.0407(2)	0.0546(6)
S1	0.1156(1)	0.5273(1)	0.04278(7)	0.0531(3)
C1	0.2962(1)	0.8970(5)	−0.0345(2)	0.0423(6)
C2	0.2909(1)	0.0613(5)	0.0545(3)	0.0488(7)
C3	0.3324(2)	0.2430(5)	0.0842(3)	0.0588(8)
C4	0.3796(2)	0.2579(5)	0.0281(3)	0.0588(8)
C5	0.3899(1)	0.0930(5)	−0.0595(3)	0.0482(7)
C6	0.4407(1)	0.1013(6)	−0.1142(3)	0.0597(8)
C7	0.4504(1)	0.9401(6)	−0.1965(3)	0.0609(9)
C8	0.4090(1)	0.7614(6)	−0.2291(3)	0.0563(8)
C9	0.3593(1)	0.7465(5)	−0.1792(3)	0.0480(7)
C10	0.3474(1)	0.9096(5)	−0.0918(2)	0.0426(6)
C11	0.2519(1)	0.7149(5)	−0.0681(3)	0.0443(6)
C12	0.1645(1)	0.3732(6)	−0.1489(3)	0.0603(8)
C13	0.0714(1)	0.7728(5)	−0.0048(3)	0.0560(8)
C14	0.0421(2)	0.7743(8)	−0.1397(4)	0.0865(1)

for 30 min), liquified Mueller Hinton agar (40–50 °C) was inoculated with the suspension of the microorganism (matched to 0.3 Mc Farland) and poured into a Petri dish to give a depth of 3–4 mm. The paper discs impregnated with the test compounds (60 μg) were placed on the solidified medium. Discs were placed on agar plates and the cultures were incubated at 37 °C for 24 h for bacteria. Inhibition zones formed on the medium were evaluated in mm. Ampicillin was chosen as a standard in antibacterial activity measurements (positive control).

3. Results and discussion

In the molecule of the title compound (Fig. 2), the bond lengths and angles are within normal ranges. Rings A (C1—C5/C10) and B (C5—C10) are planar and they are oriented at a dihedral angle of $A/B = 2.15(4)°$. So, the naphthalene ring system is nearly planar. The atoms S1, O1, N1, N2, C1, C2, C11 lie on a plane, and that plane is oriented with respect to the naphthalene ring system at a dihedral angle of 3.83(3)°. The strong intramolecular O—H...N hydrogen bond [O1—H2' 0.90(4) Å, H2'...N1 1.82(4) Å, O1...N1 2.579(4) Å and O1-H2'...N1 141(4)°] results in the formation of a non-planar six-membered ring C (C1/C2/C11/N1/O1/H2'), adopting flattened-boat [<phi> = 157.7(3)°, <theta> = 20.1(3)°] conformation, having total puckering amplitude, QT, of 1.064(3) Å [28]. The C1—C11—N1—N2 [−178.9(2)°] torsion angle shows that the configuration about the C11—N1 bond is anti (1E) [29]. On the basis of studies of intramolecular hydrogen bonds [30], a short hydrogen bond associated with a charge flow through the system of conjugated double bonds is denoted "resonance-assisted hydrogen bonding" and a delocalization parameter, $Q = (d1 - d4) + (d3 - d2)$ is defined (where the distances $d1$, $d2$, $d3$ and $d4$ are the O1—C2 [1.354(4) Å], C1—C2 [1.391(4) Å], C1—C11 [1.453(4) Å] and N1—C11 [1.274(3) Å] bond lengths, respectively). In general, the Q values have negative and positive signs in naphthaldimine and salicylaldimine derivatives, respectively, and there is no clear relationship between the corresponding Q and N...O values [31]. In contrast the Q [0.142(4) Å] value is positive in the title naphthaldimine derivative, due to the strongly electron-withdrawing nitrogen substituent group. These results related with the tautomeric form are in agreement with the other crystallographic structures [31,32]. As a result of this molecular configuration, it can be said that, 2-hydroxy-1-naphthaldehyde- N group of the molecule has distorted planar conformation. Some important bond lengths, bond angles and torsion angles to use in discussion of the molecular structure are listed in Table 3. Exact conformational knowledge can be defined by using the torsion angles about the N1—N2, N2—S1, and S1—C13

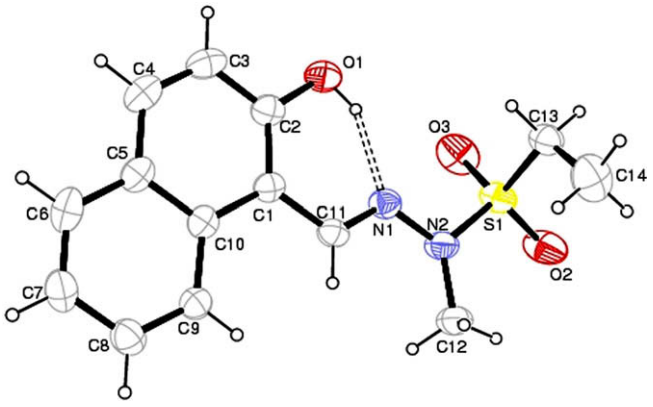

Fig. 2. The molecular structure of the title molecule with the atom-numbering scheme; displacement ellipsoids are drawn at the 50% probability level.

Table 3
Experimental and optimized geometric parameters (Å)

Parameters	X-ray analysis	B3LYP/6-31G**
The bond lengths (Å)		
O3—S1	1.433(3)	1.431
C13—C14	1.497(5)	1.520
C13—S1	1.757(3)	1.778
S1—O2	1.420(2)	1.431
S1—N2	1.644(2)	1.672
N1—C11	1.274(3)	1.259
N1—N2	1.374(3)	1.374
The bond angles (°)		
C14 C13 S1	114.2(3)	113.88
O2 S1 O3	119.60(18)	119.69
O2 S1 N2	105.47(13)	105.59
O3 S1 N2	108.00(14)	110.24
O2 S1 C13	109.48(17)	109.59
O3 S1 C13	106.85(16)	107.68
N2 S1 C13	106.80(14)	102.74
C11 N1 N2	120.4(2)	121.3
C2 C1 C10	118.3(2)	119.1
C2 C1 C11	121.2(3)	121.1
C10 C1 C11	120.4(2)	119.7
N1 N2 C12	122.7(2)	120.9
N1 N2 S1	112.24(18)	109.50
C12 N2 S1	124.1(2)	118.7
N1 C11 C1	120.3(3)	121.7
C9 C10 C5	116.8(3)	117.3
C9 C10 C1	123.6(2)	123.2
C5 C10 C1	119.6(2)	119.6
C8 C9 C10	121.8(3)	121.3
C6 C5 C4	122.4(3)	120.9
C6 C5 C10	119.3(3)	120.2

for the other part of the molecule except 2-hydroxy-1-naphthaldehyde -N group.

The geometry around S1 atom is significantly deviated from that of regular tetrahedral, similar to other reported structures [33–35]. The maximum and minimum angles around S1 are 119.6(2)° and 105.5(1)°, respectively. This distorted tetrahedral configuration probably results from the type of non-bonded interactions. Further evidence for this conclusion is provided by examination of the non-bonded contact distances [O2—O3 2.466(4), O3—N1 2.799(4), O2—C14 3.105(5) Å]. Sulfonyl atoms O2 and O3 are directed (oriented) synclinal (sc) and antiperiplanar (ap), respectively as to C14. Also O2 atom, which is involved in the smaller O—S—N angle, is synclinal (sc) to C12. The two S—O bond lengths differ by only 0.013 Å which implies that there is no delocalization of N2 lone pair into the sulfonyl group. S—O distances are similar to those found in analogous structures [36,37]. These distances do not vary significantly in the sulfonamide structure, despite the different interaction pattern observed. The S—N bond distance [1.644(2) Å] lies within expected range of 1.63–1.69 Å. In all essential details, the geometry of the molecule regarding bond lengths and angles of the compound are in good agreement with the values observed in similar structures [31–41]. Unit cell content indicating the crystal structure of the molecule is given in Fig. 3.

3.1. Computational study

To determine in vacuo conformational flexibility and the stable structures, 1D molecular energy profile of the compound was obtained with respect to the selected torsional angles varying between −180° to 180° in every 30°. For these purposes, τ_1 C14—C13—S1—N2, τ_2 C13—S1—N2—N1, τ_3 S—N2—N1—C11, τ_4 N2—N1—C11—C1 and τ_5 N1—C11—C1—C2 torsion angles were chosen. 1D potential energy scans were performed for starting with the eclipsed conformation using RHF/6-31G** method (Figs.

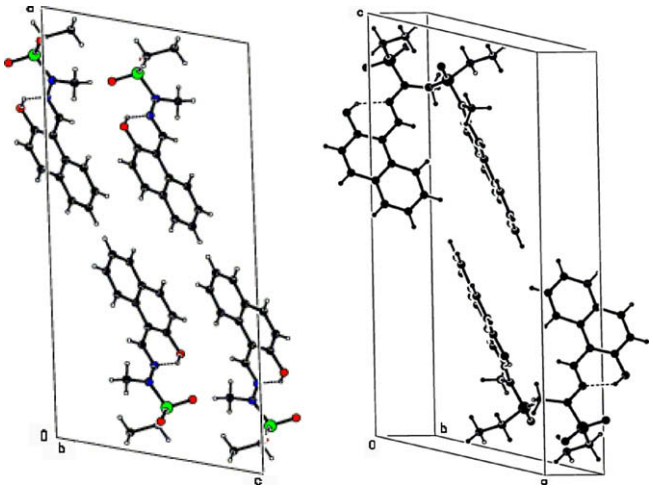

Fig. 3. Crystal packing along the *b* axis (on the left) and the best view of three dimentional unit cell perspective (on the right) of the title compound.

4 and 5). As can be seen in Figs. 4 and 5, energy profiles of τ_1 torsion shows global minima at 120°, local minima at 210°, global maxima at 320° and local maxima at 180°. τ_2 shows two local minima at about 180° and 270°, global minima at 60°, local maxima at 230° and global maxima at about 150°. Third scan for τ_3 shows global minima at 120°, global maxima at 60°, local maxima at 210°. τ_4 shows global minima at about 190°, global maxima at 90°, local maxima at about 280°. Final scan for τ_5 does not show the transition states.

Selected species were again reoptimized at DFT/B3LYP/6-31G** level and obtained result were given in Table 3. The results show good correlation with the experimental data as in salicylaldehyde sulfonylhydrazone [42]. Reoptimized conformations were given in Fig. 6. Total and relative energies of the conformers are listed in Table 4. Napthaldehyde group exists in synperiplanar (sp) in (1–7) conformers due to hydrogen bonding between N1...H1 atoms. Conformer (1) was found to be the most stable conformer in vacuo, however, conformer (5) is favored in the crystal system. The calculated difference between (1) and (5) is 2.76 kcal/mol. Changing of τ_1, τ_2 and τ_3 torsion angles caused the loss of potential energy, accompanied by changing surface area and molecular volume calculated with HyperChem 7.5 [26]. Surface area (approx) and molecular volume for conformer (1) are 451.81 Å^2 and 809.95 Å^3, however, for conformer (5) are 444.42 Å^2 and 808.61 Å^3, respectively. These results indicate that decreasing of

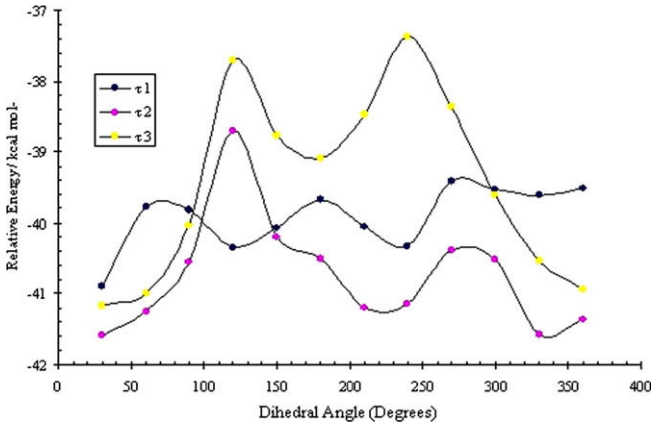

Fig. 4. The energy profile for the rotation about τ_1 C14—C13—S1—N2, τ_2 C13—S1—N2—N1 and τ_3 S1—N2—N1—C11.

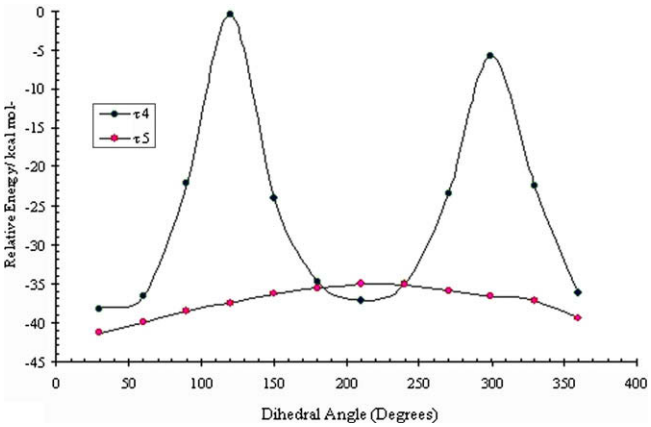

Fig. 5. The energy profile for the rotation about, τ_4 N2—N1—C11—C1 and τ_5 N1—C11—C1—C2.

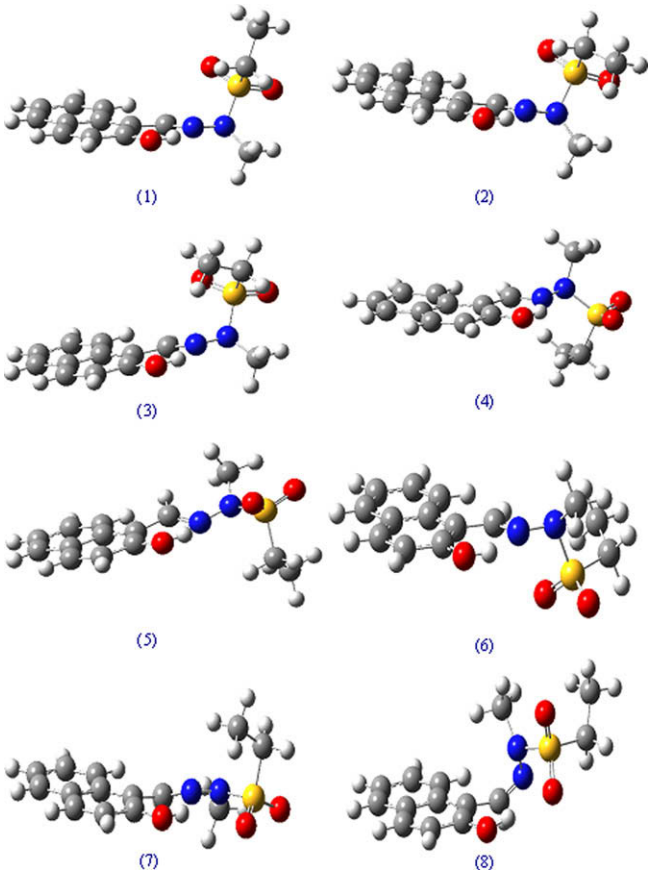

Fig. 6. Optimized geometries of conformations.

molecular volume leads to more strong intermolecular interaction or crystal packing effect, which makes conformer (5) the most stable in crystal system. These results clearly indicate that conformation was affected by intermolecular interaction in the solid phase, and it should not be neglected.

Tautomerism in 2-hydroxy Schiff bases obtained from salicylaldehyde and naphthaldehyde have been extensively studied experimentally. It is reported that phenol-imine form predominantly exist in salicylaldimine Schiff bases, however, keto-amine form is found to be dominant in naphthaldimine Schiff bases in solid state [43–45]. Keto-phenol tautomerism of the title compound is given in Fig. 7. These two tautomeric forms were optimized with BLYP/

Table 4
Total and relative energies of the conformers at B3LYP/6-31G** level

Conform	τ_1	τ_2	τ_3	τ_4	τ_5	E (a.u)	ΔE (kcal/mol)
1	−177.26	59.20	87.46	178.54	−8.09	−1270.3960	0
2	73.66	55.07	86.60	178.51	−8.63	−1270.3938	1.38
3	−74.75	68.87	85.17	178.89	−7.02	−1270.3937	1.44
4	65.05	69.02	−138.24	−178.75	−0.21	−1270.3921	2.45
5	65.38	70.41	164.25	−178.05	−2.92	−1270.3916	2.76
6	−63.12	158.57	−90.41	−179.98	−3.18	−1270.3902	3.64
7	69.14	−82.86	−165.10	177.79	−22.70	−1270.3889	4.46
8	73.15	51.83	134.76	−1.27	−63.88	−1270.3832	8.03

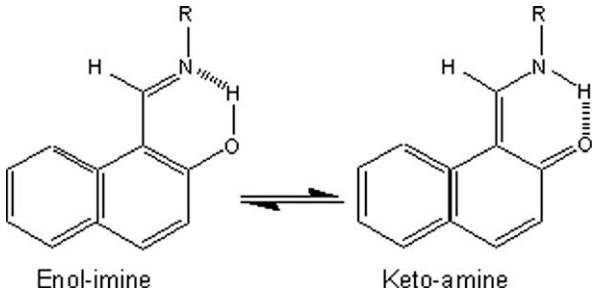

Fig. 7. Tautomerism in the title compound.

Table 5
Calculated HOMO, LUMO, heat of formation and dipole moment of tautomers

	Phenol-imine	Keto-amine
ΔE (kcal/mol)	−40.88	−18.59
μ (Debye)	3.88	1.38
HOMO/(eV)	−8.66	−8.08
LUMO//(eV)	−0.96	−1.56
ΔE (HOMO-LUMO)/eV	7.7	6.52

6-31G** level. Some physicochemical properties such as HOMO, LUMO, heat of formation and dipole moment were also calculated with the same level (Table 5). Highest negative heat of formation data shows that phenol-imine tautomer is more stable than keto-amine. On the other hand, it could be suggested that phenolic tautomer having more dipole moment should be stabilized by intermolecular interactions more than the ketonic form.

In addition, molecular hardness has been shown to be useful to rationalize the relative stability and reactivity of different species. Hard species having large HOMO-LUMO gap will be more stable and less reactive than soft species having small HOMO-LUMO gap. As can be seen in Table 5, phenol-imine tautomer has biggest hardness which explains the more stability.

Computational result is also supported by NMR data. The singlet O—H proton peak, shifting to downfield, at 10.45 ppm is indicative of the existence of intramolecular hydrogen bonding between the hydrogen atom of the hydroxyl group and imine-nitrogen atom. Furthermore, the singlet peak at 8.78 ppm belonging to the azomethine CH=N proton shows no CH—NH coupling and indicates the predominance of the phenol-imine tautomer in the title compound [46–47]. Consistence of phenol-imine tautomer in solid state was also supported by the IR spectrum of the title compound. The presence of C=N stretching vibration at 1621 cm^{-1} and the absence of N—H stretching vibration about 3300 cm^{-1} strongly suggest that the phenol-imine form is predominant tautomer in the solid state. In addition, the broad OH stretching band, shifting to lower wavenumber, at 2900 cm^{-1} can be explained by hydrogen bonding. Obtained result shows that phenol-imine form is more stable in sulfonyl hydrazone derived from 1-naphthaldehyde and sulfonamide in conformity with previous reports [40].

Table 6
Antibacterial activity of the title compound

Bacterias	Inhibitions zones (mm)	
	Compound (60 μg/disc)	Ampicillin (10 μg/disc)
E. coli ATCC 11230	11	12
P. aeruginosa ATCC 28753	10	10
S. enteritidis ATCC 40376	10	10
S. aureus ATCC 25923	9	16
B. cereus RSKK 863	8	12

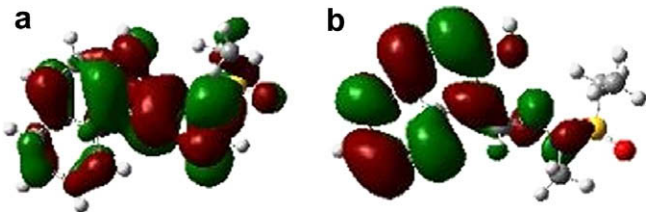

Fig. 8. Frontier molecular orbitals of title compound: (a) HOMO, (b) LUMO.

3.2. Biological evaluation

Title compound was screened for its antibacterial activity against Gram negative bacterias *E. coli* ATCC 11230, *P. aeruginosa* ATCC 28753, *S. entertidis* ATCC 40376, and Gram positive bacterias S. aureus ATCC 25923 and *B. cereus* RSKK 863. Microbiological result given in Table 6 shows that the title compound possesses a broad spectrum of activity against the tested microorganisms. It shows relatively better activity against Gram-negative than Gram-positive bacterias.

According to the molecular orbital theory, HOMO and LUMO are the most important factors affecting the bioactivity. The isosurface plots of the HOMO and LUMO are represented in Fig. 8. The LUMO of the title compound is located mainly on the aromatic ring, while the HOMO is located on the imine and ethyl groups. The interaction between the title compound and the receptor of bacteria is dominated by π–π or hydrophobic interaction among these frontier molecular orbitals. If the charge parameters are responsible for antimicrobial activity of the title compound, the negative charges mainly located on atoms O1 (−0.667), O2 (−0.686), O3 (−0.690), N1 (−0.533), N2 (−0.586) will interact with the positive part of the receptor. On the contrary, S1 (1.633) and C11 (0.357) are the most positively charged parts, which can interact with the negatively charged part of the receptor easily.

4. Supplementary data

Crystallographic data (excluding structure factors) for the structures reported in this article have been deposited with the Cambridge Crystallographic Data Centre as supplementary publication

number CCDC 683850. Copies of the data can be obtained free of charge on application to CCDC, 12 Union Road, Cambridge CB2 1EZ, UK (fax: +44 1223 336 033; e-mail: deposit@ccdc.cam.ac.uk).

Acknowledgement

This research was supported by TUBITAK Research Fund under Project No. 104T390.

References

[1] N. Anand, Burger's Medicinal Chemistry and Drug Discovery, in: M.E. Wolff (Ed.), Therapeutic Agents, fifth ed., J Wiley & Sons, New York, 1996, pp. 527–544. vol. 2.
[2] A. Peter, Netland Glaucoma Medical Therapy: Principles and Management, The American Academy of Ophthalmology, vol. 2, second ed., 2007.
[3] L. Tarko, C.T. Supuran, Bioorg. Med. Chem. 15 (2007) 5666–5671.
[4] J.Y. Winum, A. Thiry, K. El Cheikh, J.M. Dogne, J.L. Montero, D. Vullo, A. Scozzafava, B. Masereel, C.T. Supuran, Bioorg. Med. Chem. Lett. 17 (2007) 2685–2691.
[5] Z.H. Chohan, A.U. Shaikh, A. Rauf, C.T. Supuran, J. Enzyme Inhib. Med. Chem. 21 (2006) 741–748.
[6] L.L. Silva, K.N. Oliveira, R.J. Nunes, ARKIVOC 13 (2006) 124–129.
[7] L.M. Lima, E.G. Amarante, A.L.P. Miranda, C.A.M. Fraga, E.J. Barreiro, Pharm. Pharmacol. Commun. 5 (1999) 673–678.
[8] X. He, L. Tang, L. He, P. Xu, Huaxi Yike Daxue Xuebao 19 (1988) 317–319.
[9] H. Zimmer, B.H. Benjamin, E.H. Gerlach, K. Fry, A.C. Pronay, H. Schmank, J. Org. Chem. 24 (1959) 1667–1669.
[10] S. Siemann, D.P. Evanoff, L. Marrone, A.J. Clarke, T. Viswanatha, G.I. Dmitrienko, Antimicrob. Agents Chemother. 46 (2002) 2450–2457.
[11] A. Ienco, C. Mealli, P. Paoli, N. Dodoff, Z. Kantarci, N. Karacan, New J. Chem. 23 (1999) 1253–1260.
[12] N.I. Dodoff, U. Ozdemir, N. Karacan, M.C. Georgieva, S.M. Konstantinov, M.E. Stefanova, Z. Naturforsch. 54b (1999) 1553–1562.
[13] U. Ozdemir, O.S. Şenturk, S. Sert, N. Karacan, F. Ugur, Trans. Met. Chem. 28 (2003) 243–246.
[14] S. Sert, O.S. Şenturk, U. Ozdemir, N. Karacan, F. Ugur, J. Coord. Chem. 57 (2004) 183–188.
[15] U. Ozdemir, N. Karacan, O.S. Şenturk, S. Sert, F. Ugur, Synth. React. Inorg. Met-Org. Chem. 34 (2004) 1057–1067.
[16] U. Ozdemir, O.S. Şenturk, S. Sert, N. Karacan, F. Ugur, J. Coord. Chem. 59 (2006) 1905–1911.
[17] U.O. Ozdemir, G. Olgun, Spectrochim. Acta Part A, in press..
[18] O.S. Senturk, U. Ozdemir, S. Sert, N. Karacan, F. Ugur, J. Coord. Chem. 60 (2007) 229–235.
[19] O.S. Senturk, U. Ozdemir, S. Sert, N. Karacan, F. Ugur, Inorg. Chem. Commun. 6 (2003) 926–929.
[20] S. Alyar, N. Ozbek, N. Karacan, Drug Future 32 (126 Suppl. A) (2007).
[21] N. Ozbek, S. Alyar, N. Karacan, Drug Future 32 (128 Suppl. A) (2007).
[22] N. Ozbek, H. Katırcıoglu, N. Karacan, T. Baykal, Bioorg. Med. Chem. 15 (2007) 5105–5109.
[23] Cad4 Express Software Version 1.1 Delft: Enraf-Nonius, 1993.
[24] G.M. Sheldrick, SHELXS-97 and SHELXL-97, Germany:University of Gottingen, 1997.
[25] M.J. Frisch, G.W. Trucks, H.B. Schlegel, G.E. Scuseria, M.A. Robb, J.R. Cheeseman, J.A. Jr. Montgomery, T. Vreven , K.N. Kudin, J.C. Burant, J.M. Millam, S.S. Iyengar, J. Tomasi, V. Barone, B. Mennucci, M. Cossi, G. Scalmani, N. Rega, G.A. Petersson, H. Nakatsuji, M. Hada, M. Ehara, K. Toyota, R. Fukuda, J. Hasegawa, M. Ishida, T. Nakajima, Y. Honda, O. Kitao, H. Nakai, M. Klene, X. Li, J.E. Knox, H.P. Hratchian, J.B. Cross, C. Adamo, J. Jaramillo, R. Gomperts, R.E. Stratmann, O. Yazyev, A.J. Austin, R. Cammi, C. Pomelli, J.W. Ochterski, P.Y. Ayala, K. Morokuma, G.A. Voth, P. Salvador, J.J. Dannenberg, V.G. Zakrzewski, S. Dapprich, A.D. Daniels, M.C. Strain, O. Farkas, D.K. Malick, A.D. Rabuck, K. Raghavachari, J.B. Foresman, J.V. Ortiz, Q. Cui, A.G. Baboul, S. Clifford, J. Cioslowski, B.B. Stefanov, G. Liu, A. Liashenko, P. Piskorz, I. Komaromi, R.L. Martin, D.J. Fox, T. Keith, M.A. Al-Laham, C.Y. Peng, A. Nanayakkara, M. Challacombe, P.M.W. Gill, B. Johnson, W. Chen, M.W. Wong, C. Gonzalez, J.A. Pople, Gaussian, Inc., Pittsburgh PA., Gaussian 03 (Revision B.04), 2003.
[26] HyperChem 7.5 program, Hypercube Inc., Toronto, Canada, 2002.
[27] Clinical and Laboratory Standards Institute (CLSI) (formerly NCCLS), Performance Standards for Antimicrobial Disk Susceptibility Tests; Approved Standard, M02-A9. Clinical and Laboratory Standards Institute, 940 West Valley Road, Wayne, Pennsylvania, USA, 2006.
[28] D. Cremer, J.A. Pople, J. Am. Chem. Soc. 97 (1975) 1354–1358.
[29] R. Hilgenfeld, W. Saenger, Topics in Current Chemistry, in: F. Vögtle (Ed.), Springer, Verlag, New York, 1982, pp. 1–83.
[30] P. Gilli, F. Belluci, V. Ferretti, V. Bertolasi, J. Am. Chem. Soc. 111 (1989) 102–1028.
[31] T. Hökelek, S. Bilge, S. Demiriz, B. Ozguç, Z. Kılıç, Acta Cryst. C60 (2004) o803–o805.
[32] S. Sharif, D.R. Powell, D. Schagen, T. Stainer, M.D. Toney, E. Fogle, H.H. Limbach, Acta Cryst. B62 (2006) 480–487.
[33] G. Usha, S. Selvanayagama, D. Velmurugan, K. Ravikumar, P. Jaisankarc, P.C. Srinivasanc, Acta Cryst. E61 (2005). o1916–o1918.
[34] M. Ghosh, A.K. Basak, P.N. Roy, S.K. Mazumdar, Acta Cryst. C43 (1987) 732–734.
[35] S. Ozbey, A. Akbas, G. Ayhan-Kilcigil, R. Ertan, Acta Cryst. C61 (2005) o559–o561.
[36] I. Novak, W. Lib, L.J. Harrison, Acta Cryst. E63 (2007) o2599.
[37] E. Kendi, S. Ozbey, O. Bozdag, R. Ertan, Acta Cryst. C56 (2000) 457–458.
[38] A.K. Basak, Acta Cryst. C40 (1984) 419–422.
[39] M. Ghosh, A.K. Basak, S.K. Mazumdar, Acta Cryst. C43 (1987) 1552–1555.
[40] M. Ghosh, A.K. Basak, S.K. Mazumdar, Acta Cryst. C46 (1990) 1223–1226.
[41] A.K. Basak, S.K. Mazumdar, Acta Cryst. C43 (1987) 735–738.
[42] S. Alyar , O.U. Ozmen, N. Karacan, O.S. Senturk, K.A. Udachin, J. Mol. Struct, in press..
[43] T. Hökelek, Z. Kılıç, M. Işıklan, M.J. Toy, Mol. Struct. 523 (2000) 61–69.
[44] H. Nazır, M. Yıldız, H. Yılmaz, M.N. Tahir, D. Ulku, J. Mol. Struct. 524 (2000) 241–250.
[45] M. Yıldız, Z. Kılıç, T. Hökelek, J. Mol. Struct. 441 (1998) 1–10.
[46] S.G. Öztas¸, E. Sahin, N. Ancın, S. Ide, M. Tuzun, Z. Kristallogr. 218 (2003) 492–496.
[47] N. Ancın, O. Celik, S.G. Oztas, S. Ide, Struct. Chem. 18 (2007) 347–352.